Fatty Acid−Albumin Complexes and the Determination of the Transport of Long Chain Free Fatty Acids across Membranes†

David Cupp, J. Patrick Kampf, and Alan M. Kleinfeld*

Torrey Pines Institute for Molecular Studies, 3550 General Atomics Court, San Diego, California 92121

Received December 30, 2003; Revised Manuscript Received February 14, 2004

ABSTRACT: Understanding the mechanism that governs the transport of long chain free fatty acids (FFA) across lipid bilayers is critical for understanding transport across cell membranes. Conflicting results have been reported for lipid vesicles; most investigators report that flip-flop occurs within the resolution time of the method (<5 ms) and that dissociation from the membrane is rate limiting, while other studies find that flip-flop is rate limiting and on the order of seconds. We have reinvestigated this problem and find that the methods used in studies reporting rapid flip-flop have not been interpreted correctly. We find that accurate information about transport of FFA across lipid vesicles requires that FFA be delivered to the vesicles as complexes with albumin (BSA). For example, we find that stopped-flow mixing of uncomplexed FFA with small unilamellar vesicles (SUV) containing pyranine yields the very fast influx rates reported previously (>100 s^{-1}). However, these influx rates increase linearly with lipid vesicle concentration and can therefore not, as previously interpreted, represent flip-flop. In contrast, measurements of influx rates in SUV and giant unilamellar vesicles performed with oleate−BSA complexes reveal no dependence on vesicle concentration and yield influx rate constants of ∼4 and ∼0.5 s^{-1}, respectively. Rate constants for efflux and dissociation were determined from the transfer of oleate from vesicles to BSA and reveal similar influx and efflux but dissociation rate constants that are ∼5−10-fold greater. We conclude that flip-flop is rate limiting for transport of FFA across lipid vesicles and slows with an increasing radius of curvature. These results, in contrast to those reporting that flip-flop is extremely fast, indicate that the lipid bilayer portion of biological membranes may present a significant barrier to transport of FFA across cell membranes.

Transport of long chain free fatty acids (FFA)[1] across membranes is a necessary step for utilization of FFA. Although considerable effort has been devoted to understanding the mechanism of transport, substantial disagreement about whether transport is facilitated by membrane proteins or occurs by diffusion through the lipid phase remains. A protein-mediated mechanism would necessitate slow diffusion across the lipid phase, and therefore, understanding the mechanism of transport across simple lipid membranes has received considerable attention (*1*−*4*). The focus of previous studies has been to determine which step in the transport process is rate limiting: the off step or flip-flop. The binding step in these studies was not thought to be rate limiting.

As far as we know, virtually all previous studies, except our own, have reported extremely fast rates for transport of native FFA across lipid membranes, implying that the bilayer presents a negligible barrier to flip-flop (*5*−*10*). In the two most recent studies, stopped-flow measurements were taken using vesicles containing the pH sensitive fluorophore, pyranine (*7*, *9*). The rate of flip-flop was determined from the rate of change of pyranine fluorescence after vesicles were mixed with native long chain FFA not complexed with BSA and after the extravesicular pH was altered in vesicles containing FFA. The time required for the change in pyranine fluorescence was generally found to be shorter than the stopped-flow resolution (<5 ms) (*7*, *9*).

In our previous study of the transport of native long chain FFA across lipid vesicles, we also mixed, by stopped-flow, uncomplexed FFA with vesicles containing trapped ADIFAB or pyranine (*11*). These vesicles were composed of egg phosphatidylcholine (EPC) and cholesterol and were large (LUV) or giant (GUV) unilamellar vesicles but not the small unilamellar vesicles (SUV) used in most of the studies reporting rapid flip-flop. We reported flip-flop times that were significantly slower (>100-fold) than the stopped-flow resolution of 5 ms. However, we noted that very fast rates (>100 s^{-1}) were often observed at the most rapid stopped-flow rates, especially with vesicles composed of EPC without cholesterol. In studies using uncomplexed FFA, the initial FFA concentration generally exceeds 1 μM. We speculated that these high concentrations in the context of rapid stopped-flow mixing might perturb the bilayer structure and result in anomalously high rates of transbilayer transport of FFA.

† This work was supported by Grant DK058762-03 from the National Institute of Diabetes and Digestive and Kidney Diseases.

* To whom correspondence should be addressed. Telephone: (858) 455-3724. E-mail: akleinfeld@tpims.org.

[1] Abbreviations: ADIFAB, acrylodan-labeled intestinal fatty acid binding protein; EPC, egg phosphatidylcholine; FFA, nonesterified fatty acids bound or unbound in the aqueous phase; GUV, LUV, and SUV, giant, large, and small unilamellar vesicles, respectively; k_{ff} and k_{off}, flip-flop and dissociation rate constants, respectively; k_{in}, k_{out}, and k_{trns}, empirical rate constants for influx, efflux, and vesicle to protein transfer, respectively; OA, oleate.

10.1021/bi036335l CCC: $27.50
Published on Web 03/25/2004

Therefore, in a subsequent study of erythrocyte ghosts, FFA were added as complexes with BSA (*12*).

The results of our previous studies raised the possibility that rapid stopped-flow mixing of uncomplexed FFA with vesicles might induce transient defects across the bilayer that would result in anomalously fast rates of transport. Because these studies also suggested that such an effect would be prevented if FFA were delivered as complexes with BSA, we have in the study presented here investigated transport of oleate across SUV as well as GUV using stopped-flow mixing in which FFA were delivered to the vesicles as complexes with BSA. We have also further investigated the characteristics of the three types of experiments that were used to infer rapid flip-flop: stopped-flow mixing with uncomplexed oleate, pH-jump measurements, and inter-vesicle transfer of FFA. The results indicate that these types of measurements do not provide information about flip-flop. We conclude, in contrast to previous studies, that flip-flop is rate limiting in lipid vesicles and that flip-flop of long chain FFA through the lipid phase of biological membranes probably represents a significant barrier to cellular transport of FFA.

EXPERIMENTAL PROCEDURES

Materials. Egg phosphatidylcholine (EPC) and bovine phosphatidylserine (PS) were purchased from Avanti Polar Lipids, Inc. (Alabaster, AL), and [*choline-methyl*-^{3}H]-L-α-dipalmitoylphosphatidylcholine (DPPC) was from American Radiolabeled Chemicals, Inc. (St. Louis, MO). Sodium oleate (OA) was purchased from NuChek Prep (Elysian, MN), and stock solutions were prepared in water containing 4 mM NaOH (pH 11) and 50 μM butylated hydroxytoluene. Pyranine (8-hydroxypyrene-1,3,6-trisulfonic acid) was purchased from Molecular Probes (Eugene, OR). ADIFAB was prepared as described previously (*13*) and is available from FFA Sciences LLC (San Diego, CA). Fatty acid free BSA was purchased from Sigma-Aldrich (St. Louis, MO). Recombinant intestinal fatty acid binding protein (I-FABP) was prepared as described previously (*13*).

The buffer used in FFA transport experiments involving BSA contained 20 mM Hepes, 140 mM NaCl, and 5 mM KCl at pH 7.4 (buffer A), and both the OA−BSA complexes and vesicles were prepared in this buffer. In the absence of BSA (uncomplexed OA), OA in either 150 mM NaCl, 5 mM KCl, 4 mM NaOH (pH 11) (isotonic), or 4 mM NaOH (pH 11) was mixed with vesicles in buffer A. Equivalent results were obtained with either OA solution.

Vesicle Preparation. Vesicles were prepared as described previously (*11, 14*). Films of EPC were produced by rotary evaporation of chloroform solutions containing 44 μmol of EPC and 5 μCi of [^{3}H]dipalmitoylphosphatidylcholine (DPPC). The film was sealed with argon and lyophilized overnight. Small unilamellar vesicles (SUV) were prepared by sonication of the lipid film hydrated in 2 mL of buffer A. For vesicles in which pyranine was trapped, 0.5, 2, or 20 mM pyranine (virtually identical results were obtained for all three concentrations) was included in the buffer. Vesicles were sonicated for 15−30 min at 60−70 W using a Branson sonicator. The sonicated suspension was centrifuged for 45 min at 12000*g*; the supernatant was dialyzed in 4 L of buffer A for 12 h at 4 °C and chromatographed on Sephacryl S-1000 to separate remaining free and trapped pyranine. Large unilamellar vesicles (LUV) were prepared by extrusion as described previously (*11*).

Giant unilamellar vesicles (GUV) were prepared by dialysis of 1−2 mL of octyl β-glucopyranoside (OG)-solubilized EPC using SpectraPore 4 (3500 Da cutoff) dialysis tubing as described previously (*11*). Trapping was done by including either 400 μM ADIFAB or 20 mM pyranine in the OG solution. Because pyranine can diffuse through the dialysis tubing, pyranine-containing solutions were first dialyzed against a 10−20-fold volume of buffer A which allows vesicles to form while maintaining a significant level of trapped pyranine. Dialysis was continued at 4 °C against four buffer changes of 4 L each over the course of 4 days. Following dialysis, the suspension was centrifuged at 330*g* for 5 min and was then chromatographed on Sephacryl S-1000.

Sephacryl S-1000 elution profiles for both SUV and GUV were monitored by [^{3}H]DPPC activity and fluorescence, in preparations with trapped fluorophore. Phospholipid concentrations were determined for (1) unfractionated vesicles (after sonication or dialysis but before centrifugation or chromatography), (2) vesicles that pelleted at 330*g*, and (3) vesicles that eluted from the Sephacryl S-1000 column. The phospholipid concentration was determined using the Elon method for total inorganic phosphate (*15*). Vesicle concentrations used in the stopped-flow experiments ranged from 2.5 to 250 μM. All stopped-flow concentrations refer to values in the mixing chamber, not in the syringe.

Oleate−BSA Complexes and Buffering of Unbound Oleate. Complexes of oleate (OA) and BSA were prepared so that unbound OA (OA_u) concentrations were buffered at defined values. The complexes were prepared by mixing aliquots of OA from a 5 mM stock solution in 4 mM NaOH at 37 °C with a 600 μM BSA solution in buffer A, also at 37 °C. The concentration of free or unbound OA was monitored several times during this titration using ADIFAB (*16*), and the final OA_u concentration ranged from 5 nM to 1.5 μM. A critical feature of the OA−BSA complexes is that at sufficiently high BSA concentrations, the OA_u concentration will not change upon addition of vesicles. The conditions for a well-buffered system depend on the OA_u, BSA, and vesicle concentrations and are determined by ensuring equal values of the OA_u concentration in the complex and complex with vesicles through direct measurement with ADIFAB. For a well-buffered system, and at a sufficiently low OA_u concentration, the influx time courses are described well by a single exponential. However, for a poorly buffered system, the influx time course reveals additional temporal components, both faster and slower than those observed with the well-buffered system.

Fluorescence Instrumentation. The kinetics of FFA movement was monitored by stopped-flow mixing with a temporal resolution of <5 ms and by a slow-mixing method with a resolution of <200 ms. Stopped-flow fluorescence was assessed using a Kintek Instrument (State College, PA) apparatus in which equal volumes of 0.05 mL reactants were mixed at flow rates of ≥6 mL/s as described previously (*11*). All concentrations refer to the value in the mixing chamber. Tryptophan, ADIFAB, and pyranine fluorescence intensities were monitored by exciting the sample at 290, 386, and 445

nm, respectively, and observing emission through 20 nm bandwidth filters at 343, 432, and 505 nm, respectively. At least two separate preparations and three kinetic traces were generated for most experimental conditions.

The results of this study raise the possibility that rapid mixing and possibly hydrodynamic forces generated by stopped-flow mixing perturb lipid vesicles and thereby distort the kinetics of the OA−vesicle interaction. We therefore devised a system that would mix oleate and GUV faster than the influx rate but more slowly (and presumably more gently) than stopped-flow mixing. To do this, we used a Hamilton Microlab 500 series titrator that was interfaced with a cuvette placed in a magnetically stirred thermostatic cell holder of a Spex Fluorolog 3 fluorometer. A measurement was initiated by filling the cuvette with ~2 mL of a suspension of pyranine containing GUV in buffer A, placing the tubing from the titrator into the buffer, initiating data collection, and injecting 20 μL of uncomplexed oleate or 40 μL of the OA−BSA complex into the GUV suspension. The fluorescence (445 nm excitation and 505 nm emission with 2 and 4 nm bandpasses, respectively) was monitored for 10−20 s, integrating for 6 ms, every 9 ms. The titrator required less than 20 ms to inject 20 μL (flow rate of 1 mL/s). The mixing time of the system was determined by monitoring the time course of pyranine fluorescence upon injecting 20 μL of water at pH 0.5 into 2 mL of 10 μM pyranine in buffer A.

Transfer of Oleate between Vesicles and Proteins. SUV and GUV were loaded with OA by titrating a rapidly stirring solution of vesicles with aliquots of sodium oleate. Titrating the vesicles with OA was done by diluting a 50 mM NaOA solution to 500 μM in 4 mM NaOH (pH 11), increasing the temperature to 37 °C, and distributing equal aliquots, waiting 2 min between aliquots, into a rapidly stirring solution. For efflux and protein transfer experiments, lipid concentrations ranged from 5 to 250 μM and the fraction of OA ranged from 1 to >40 mol % lipid. Acceptor proteins were BSA, used between 5 and 150 μM, and I-FABP, used between 4 and 50 μM. More than 200 efflux/transfer and more than 150 influx experiments were performed.

Analysis of OA Kinetics. Three different time courses were measured in this study: (1) influx measurements in which the time course of the movement of OA from the BSA donor to the vesicles was monitored by the fluorescence from pyranine and/or ADIFAB trapped within the vesicle, (2) efflux measurements in which the time course of the movement of OA from the vesicles to a protein in the extravesicular region was monitored by trapped pyranine and/or ADIFAB, and (3) transfer measurements in which the movement of OA from the vesicles to an extravesicular protein was monitored by the change in the protein fluorescence. The kinetic traces were fitted with multiexponential functions to determine empirical rate constants for influx (k_{in}), efflux (k_{out}), and vesicle to protein transfer (k_{trns}).

To determine the intrinsic rate constants for flip-flop (k_{ff}) and dissociation (k_{off}) that govern the time courses and to better understand their dependence on kinetic parameters, we used the analysis and simulation facilities of MLAB (Civilized Software, Bethesda, MD) and MACSYMA. In the study presented here, we have extended our previous methods of analysis (*11*) to simultaneously fit all three time courses using a modification of the kinetic model from our previous study. This model accounts for the movement of OA between BSA and vesicles and the movement of OA across the bilayer. Details of the model are provided in the Appendix.

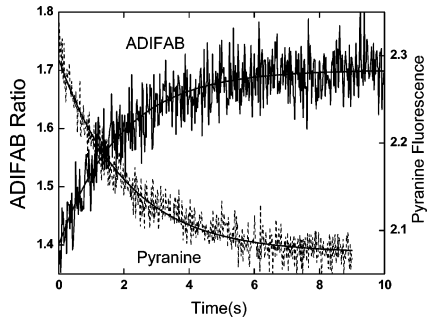

FIGURE 1: Influx of oleate for GUV using the OA−BSA complex. Fluorescence time courses from stopped-flow mixing (unless otherwise indicated, all time courses were determined by stopped-flow mixing) of the OA−BSA complex with GUV with trapped pyranine or ADIFAB. For ADIFAB, the ratio of emission intensities at 505 nm to those at 432 nm is plotted. The GUV concentration was 250 μM with ADIFAB and 50 μM with pyranine; the BSA concentration was 25 μM, and the OA_u concentration was 40 nM. Single-exponential fits yielded rate constants of 0.53 s^{-1} for ADIFAB and 0.48 s^{-1} for pyranine. The experimental results and analysis shown here and in the other figures are representative examples of at least three separate experiments.

RESULTS

Influx Rate Constants Measured with the OA−BSA Complex Are Slow. Stopped-flow measurements were taken to determine the rate constants for the transfer of oleate from the outer aqueous phase to the inner hemileaflet of EPC-GUV. OA−BSA complexes, whose OA_u concentrations were determined by direct measurement, were mixed with GUV containing either the pyranine or ADIFAB fluorescent probe. Results for both pyranine and ADIFAB revealed rate constants of ~0.5 s^{-1} (Table 1 and Figure 1). As discussed in the Appendix, influx is not rate limited by dissociation of OA from BSA. Influx rate constants were independent of GUV concentration (5−50 μM with a BSA concentration of 25 μM and an OA_u concentration of 37 nM) and BSA concentration (25−200 μM with a GUV concentration of 85 μM and an OA_u concentration of 95 nM), suggesting that the rate-limiting step is first-order (data not shown). Although influx rate constants reveal no dependence on GUV or BSA concentration for a fixed OA_u concentration, influx rate constants were found to increase with an increase in the OA_u concentration (Figure 2). Additional results presented in the following sections suggest that this change in rate constant reflects perturbation of the bilayer by oleate.

Similar measurements were taken using EPC-SUV containing pyranine and revealed k_{in} values that were ~10-fold faster (4 s^{-1}) than that for GUV (Figure 3). As in the case of GUV, the influx rate constants revealed (data not shown) no dependence on SUV concentration (10−250 μM) or BSA concentration (0.5−50 μM). However, just as for GUV, SUV influx rate constants reveal increases with an increase in OA_u concentration, at least for values greater than 50 nM (Figure 2). Moreover, except for results at ≤50 nM OA_u, the time courses are described well by two exponentials with a k_{slow} of 4 s^{-1} and k_{fast} of 23 s^{-1}. The increase in the overall rate constant is due to the growing contribution of the fast component (see the inset of Figure 2).

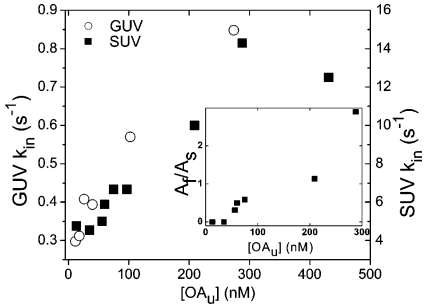

FIGURE 2: OA_u concentration dependence of influx rate constants. Influx rate constants were determined, as described in the legend of Figure 1, for both SUV and GUV with OA−BSA complexes that generated increasing OA_u concentrations. In these experiments, the fluorescence was monitored from pyranine trapped in SUV and GUV, with EPC concentrations of 5 and 50 μM and BSA concentrations of 25 and 12.5 μM, respectively. The inset shows the ratio of the fast to slow component amplitudes for a two-exponential fit for the SUV results.

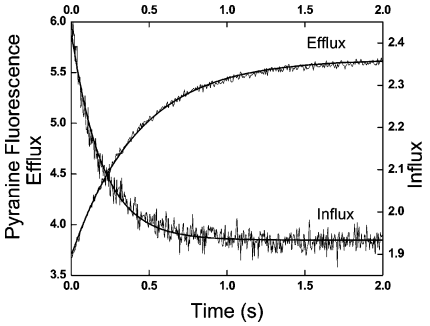

FIGURE 3: Influx (OA−BSA) and efflux of oleate with SUV. The trapped pyranine fluorescence was used to monitor influx (50 μM SUV, 25 μM BSA, and 60 nM OA_u) and efflux (250 μM SUV, 25 μM OA_T, and 25 μM BSA). The single-exponential fits to these time courses yielded rate constants of 5 and 2.3 s^{-1} for influx and efflux, respectively.

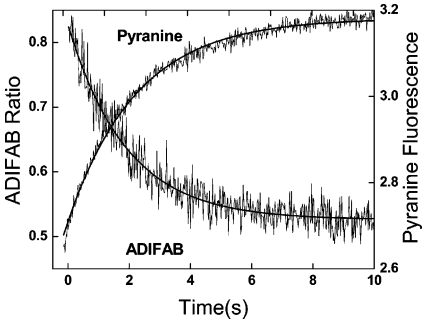

FIGURE 4: Efflux of oleate from GUV. Measurements were taken by monitoring the fluorescence from trapped pyranine or ADIFAB after mixing with BSA. For pyranine, 50 μM GUV, 5 μM OAB_{TB}, and 37 μM BSA were used, and for ADIFAB, 100 μM GUV, 10 μM OA_T, and 25 μM BSA were used. Single-exponential fits yielded k_{out} values of 0.3 and 0.5 s^{-1} for pyranine and ADIFAB, respectively.

Oleate Efflux Rates Are Similar to Influx Rates. Measurements of the rate of oleate efflux were done by stopped-flow mixing of oleate-loaded donor vesicles with fatty acid free BSA. For GUV, both pyranine and ADIFAB time courses revealed equivalent values for k_{out} (0.4 s^{-1}) (Figure 4). Similar efflux rate constants were obtained using a GUV concentration of 50 or 100 μM and BSA concentrations from 5 to 38 μM (data not shown). Efflux measurements for SUV revealed a k_{out} of ~2 s^{-1} (Figure 3) and a similar lack of dependence on SUV concentration, acceptor type, and BSA

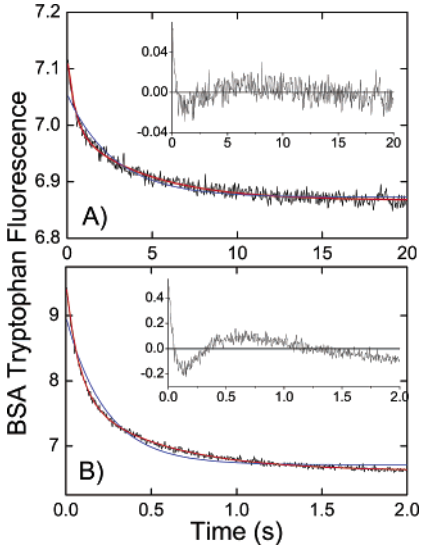

FIGURE 5: Transfer of oleate from vesicles to BSA. Transfer of oleate from donor vesicles to BSA was monitored by the change in the BSA tryptophan fluorescence upon binding oleate. (A) For GUV, 250 μM GUV, 25 μM OA_T, and 38 μM BSA were used. The double-exponential fit (red line) yields rate constants of 2.2 and 0.23 s^{-1} which are equal in amplitude, and the single fit (blue line) yields a value of 0.4 s^{-1} and a significantly poorer fit as indicated by the residuals in the inset. (B) For SUV, 105 μM SUV, 20 μM OA_T, and 10 μM BSA were used. The double fit yields rates of 11.4 (59%) and 2 s^{-1} (41%), respectively, and the single fit yields a rate of 4.2 s^{-1}.

concentration as for GUV (data not shown). SUV rate constants increased significantly for oleate/SUV ratios of >20 mol % (data not shown). The sensitivity of efflux to oleate concentration is also consistent with the influx results and provides additional evidence that high oleate concentrations perturb bilayer properties. For both SUV and GUV, influx and efflux rate constants were similar, consistent with the notion that these rates reflect oleate flip-flop. An independent measurement of the dissociation of oleate from the vesicles is required, however, to determine if efflux primarily reflects flip-flop or dissociation.

Dissociation of Oleate from Vesicles Is Faster than Efflux. Measurements of the transfer of oleate to protein (dissociation) were taken using the same experimental configuration and vesicles that were used for efflux, except that the acceptor protein's tryptophan fluorescence was monitored, rather than that of the internal pyranine or ADIFAB. Results for GUV reveal time courses that require two exponential components: a fast component of ~3 s^{-1} and a slower component of ~0.3 s^{-1} (Figure 5A). This suggests that the slow rate constant, which is similar to the rate constants determined from influx and efflux measurements, represents flop-flip. This interpretation is supported by modeling of the transfer of OA from vesicles to BSA using eqs 1−4 of the Appendix. These simulations (not shown) reveal, for slow flip-flop and fast dissociation, a time course virtually identical to those that have been observed (Figure 5, for example). In contrast, a process involving rapid flip-flop and slow dissociation yields a monoexponential time course with a rate constant of much less than k_{off}^{M} (for either mechanism, there is little to no dependence on BSA rate constants). Thus, the measurements of the transfer of oleate from GUV to BSA indicate that transfer to BSA occurs first by rapid dissociation from the outer leaflet of the GUV followed by a more than

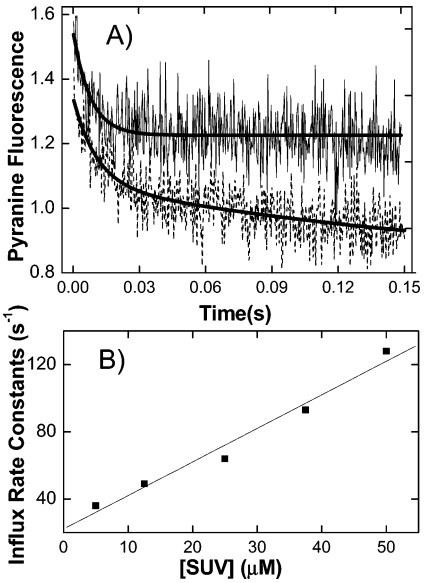

FIGURE 6: Uncomplexed oleate and SUV. Oleate in 150 mM NaCl and 5 mM KCl at pH 11 was stopped flow mixed with pyranine-containing SUV. (A) Time courses for 5 and 50 μM SUV and 2 μM OA_T. Single-exponential fits yielded rate constants of 36 and 91 s^{-1} for the 5 and 50 μM SUV, respectively. (B) Influx rate constants with increasing SUV concentrations. A linear fit using $k_{in} = k_{off} + k_{on}$[SUV] yields a k_{on} of 3×10^6 M^{-1} s^{-1} and a non-zero intercept from which $k_{off} = 13.4$ s^{-1}.

10-fold slower flip-flop of oleate across the bilayer and, therefore, that flip-flop is rate limiting for GUV.

Similar methods were used to monitor dissociation of oleate from SUV. The results also reveal a two-component time course in which the major component equals ~13 s^{-1} and the slow component ~2 s^{-1} (Figure 5B). The value of 13 s^{-1} is in excellent agreement with the results of Pownall and co-workers, whose results indicate a rate constant for dissociation of OA from SUV of ~12 s^{-1} at 24 °C (*17*). The slow component of Figure 5B is virtually identical to the measured efflux rate constants. This indicates, just as for GUV, that the transfer of oleate from SUV to BSA consists first of rapid dissociation from the outer hemileaflet followed by a more than 6-fold slower flop-flip and, therefore, that flip-flop is the rate-limiting step for the transport of oleate across SUV.

Influx with Uncomplexed Oleate Is Fast. The influx results with OA−BSA complexes as well as efflux measurements are consistent with flip-flop times on the order of seconds but are inconsistent with studies done with uncomplexed FFA which reveal influx times of <5 ms (*7*, *9*). We have confirmed these much faster influx times in stopped-flow measurements using uncomplexed oleate mixed with pyranine-containing SUV (Figure 6A) and GUV containing pyranine or ADIFAB (data not shown). However, as indicated by the results in Figure 6, the observed influx rates are vesicle concentration-dependent; k_{in} increases with an increase in SUV concentration. An investigation of this dependence for SUV reveals that k_{in} increases linearly with an increase in SUV concentration, so k_{in} ranges from 35 s^{-1} for 5 μM SUV to >120 s^{-1} for >50 μM SUV (Figure 6B).

These fast rates are difficult to reconcile with FFA flip-flop. First, flip-flop is a first-order process, and therefore, the observed rate should be independent of vesicle concentration. The linear dependence on SUV concentration suggests that the pyranine response reflects the binding of OA to the vesicle, rather than the translocation step. This follows because, as discussed in the Appendix, the solution for FFA binding to the outer hemileaflet of the bilayer yields a linear dependence on SUV concentration for the binding rate constant ($k_{binding} = k_{off} + k_{on}$[SUV]). Rate constants derived from a fit of this expression to the data of Figure 6B are in good agreement with independent determinations of these quantities. For example, the k_{off} value (14 ± 3 s^{-1}), determined from measurements such as that shown in Figure 6B, is in good agreement with k_{trns} (13 ± 2 s^{-1}). In addition, the value for k_{on} (~3×10^6 M^{-1} s^{-1}) obtained from this fit is in good agreement with the k_{on} (4.5×10^6 M^{-1} s^{-1}) determined from the measured K_p (4×10^5) for oleate (*18*) and k_{off} ($0.8K_p \approx k_{on}/k_{off}$). Second, influx time courses for uncomplexed OA with GUV, measured using ADIFAB or pyranine, yield fast (>14 s^{-1}) rate constants. Because the ADIFAB response requires dissociation of oleate from the inner leaflet and because the dissociation rate constant for GUV is 3 s^{-1}, influx with uncomplexed oleate appears to bypass the flip-flop and dissociation steps.

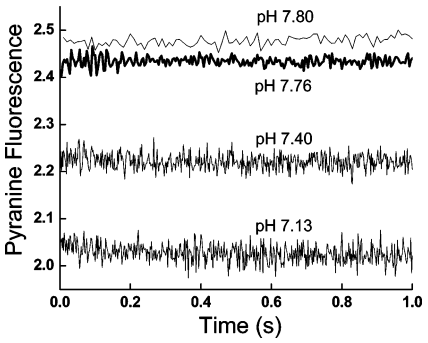

FIGURE 7: Lack of oleate dependence of the SUV pH response. Stopped-flow mixing of SUV (133 μM at pH 7.4) with HEPES buffer at lower or higher pH_o so that the final pH of the mixture is between 7.1 and 7.8 (see the figure). The fluorescence of trapped pyranine with *no added oleate* reveals an approximately ±10% change with a changing pH_o (results for 0 mol % OA are depicted with thin lines). Addition of 2, 4, or 6 mol % OA does not affect the pH_i response as indicated by the thick line at pH 7.76 which is the result for 6 mol % oleate (2 and 4% are virtually identical to 6 mol %).

pH_o-Jump Measurements Reveal that Rapid pH_i Changes Are Independent of OA Loading of SUV. Monitoring pH_i after changing pH_o has been proposed as an alternative method of determining flip-flop (*7*, *9*). The results of these measurements reveal pH_i changes that occur in less than 5 ms. However, these changes do not appear to be correlated with the concentration of OA in the vesicle (*15*). We investigated this lack of OA concentration dependence directly by measuring the pyranine time course in SUV containing 0−6 mol % oleate, after changing the pH_o. As observed in previous studies (*7*, *9*), the pH_i time course was too rapid to be resolved by stopped flow (Figure 7). However, this pH_i change was not dependent on oleate concentration, and the same ΔpH_i was observed for 0−6 mol % OA. (In contrast, fluorescence changes for both the efflux and transfer processes were dependent on OA concentration.) We were able to reduce this pH_i change by addition of BSA, suggesting that an impurity in the SUV was at least partially responsible for the rapid ΔpH_i. In addition, ~30% of the pyranine fluorescence, in pyranine-containing SUV, could be quenched with the nonpermeable reagent *p*-xylene bispy-

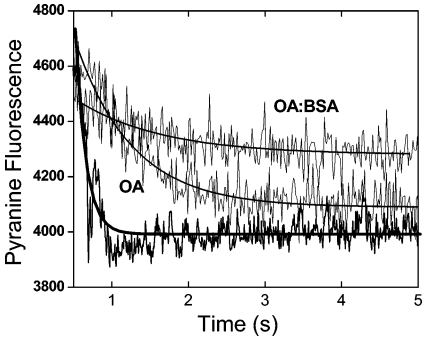

FIGURE 8: Influx of oleate into GUV by slow mixing. Two milliliters of pyranine GUV (50 μM) was mixed with OA using the slow-mixing apparatus (Experimental Procedures). Rate constants for the decay of pyranine fluorescence were obtained by single-exponential fits (depicted with solid lines). The curve labeled OA:BSA was obtained by adding the OA−BSA complex (0.04 mL of a 625 μM solution) to the GUV so that the final BSA concentration was 12.5 μM and the OA_u concentration was 26 nM; the fit yielded a k_{in} of 0.9 s^{-1}. The curve labeled OA was obtained by adding 0.02 mL of 500 μM oleate (pH 11, final concentration of 5 μM) to the GUV and yielded a k_{in} of 1.4 s^{-1}. The third curve (mixing rate control) was obtained by adding 0.02 mL of 0.65 pH HEPES to 10 μM pyranine in pH 7.4 HEPES and yielded a k of 7.1 s^{-1}.

ridinium bromide (DPX). This is consistent with the observations of Barreto and Lichtenberg (*19*), who described the presence of extravesicular pyranine and characterized its quenching by DPX. These results indicate that a significant fraction of the SUV-associated pyranine is accessible to the extravesicular phase and might therefore contribute to the rapid pH change.

Slow Mixing. These results, as well as our previous studies (*11*, *12*), suggest that the fast influx rates observed with uncomplexed OA may be due to a perturbation of the bilayer. This may result from rapid loading of the outer hemileaflet with high concentrations of OA, perhaps augmented by hydrodynamic forces generated by stopped-flow mixing. To test this possibility, we monitored influx using a mixing system that allows uncomplexed oleate and vesicles to be mixed in a cuvette with mixing times of <0.2 s (see *Slow Mixing* in Experimental Procedures). This mixing is slower than stopped flow but is faster than the time of influx observed for GUV with the OA−BSA complex (2 s). Slow mixing measurements with pyranine-containing GUV mixed with uncomplexed oleate reveal a rate constant of ~1.4 s^{-1} (Figure 8), somewhat faster than the value obtained by stopped flow with the OA−BSA complex but more than 10-fold slower than that from stopped flow with uncomplexed OA. These results are consistent with the notion that the fast rate observed by stopped-flow mixing with uncomplexed oleate is due to the perturbations induced by rapid (<5 ms) exposure of the vesicles to high levels of OA.

The Presence of Anionic Phospholipids Does Not Alter Transport Rates. To begin to evaluate the role of lipid components other than phosphatidylcholine, we measured transport across lipid vesicles containing the negatively charged lipid, phosphatidylserine (PS). We determined influx and efflux rate constants using SUV and LUV (both 100% EPC and EPC with 8% PS). Rate constants for 8% PS SUV were 4.1 and 1.7 s^{-1} for influx and efflux, respectively, virtually identical to the values in pure EPC (Table 1). For LUV, k_{in} was 0.6 s^{-1} for EPC and 0.8 s^{-1} for 8% PS, while

Table 1: Observed Rate Constants[a]

	k_{in} (s^{-1})	k_{out} (s^{-1})	k_{trn} (s^{-1})
SUV	4 ± 1	2.0 ± 0.4	13 ± 2
GUV	0.5 ± 0.1	0.4 ± 0.1	3 ± 1

[a] Averages and standard deviations from at least two different vesicle preparations and four separate experiments each, and each of these consisted of at least two scans each.

the k_{out} values were 0.4 and 0.6 s^{-1}, respectively (uncertainties of ~0.1 s^{-1}). These results indicate that the presence of negative surface charge has little effect on FFA transport. The presence of surface charge may reduce the pH near the surface, relative to that of the bulk solution, thereby increasing the rate of protonation of the FFA anion and thus the influx rate. On the other hand, an FFA anion experiences a repulsive interaction from the negative surface potential. Indeed, the partition coefficient for the anion is substantially reduced in charged as compared to neutral vesicles (*20*). Thus, the lack of a surface charge effect may result because of these compensatory effects and/or because protonation and deprotonation steps are significantly faster than flip-flop. The lack of surface charge effects in lipid vesicles is also consistent with measurements in erythrocyte ghosts for which transport rates are quite similar to those of EPC-GUV (*12*).

DISCUSSION

The results of this study reveal that flip-flop is the rate-limiting step for the transport of oleate across lipid bilayer membranes; flip-flop is 5−10-fold slower than dissociation. In contrast, previous studies have reported that flip-flop is extremely fast and that dissociation is the rate-limiting step for the transport of long chain FFA across lipid membranes (*5*−*10*, *21*). The evidence for rapid flip-flop was derived from three types of measurements: (1) FFA influx using uncomplexed FFA, (2) transfer of FFA between vesicles, and (3) pH-jump measurements of FFA-containing vesicles. In this study, we demonstrated that the interpretation of the results of these three types of experiments in terms of flip-flop was inaccurate.

First, we showed that measurements taken using uncomplexed FFA cannot represent flip-flop because they reveal second-order kinetics (Figure 6).[2] We also provided evidence that measurements with uncomplexed FFA cannot be used to measure transport properties because this procedure perturbs vesicle characteristics. Second, we showed that the interpretation of the rate constant for intervesicle transfer as the dissociation rate constant was incorrect. Direct measurements of dissociation rate constants, by ourselves and previously by Pownall and co-workers (*17*), reveal values that are 5−10-fold faster than the rates of intervesicle

[2] In our previous study of transport across lipid vesicles, we also used uncomplexed FFA but reported slow flip-flop for cholesterol-containing LUV and GUV (*11*). Slow rates, as compared to that of EPC-SUV, may in part be due to the presence of cholesterol in the larger vesicles. The slow rates may also be a reflection of the decrease in apparent influx rates with decreasing vesicle concentration, when using uncomplexed FFA, and the low vesicle concentrations (40 μM) used in the study. Thus, our previous report (*11*) of slow flip-flop in lipid vesicles may be inaccurate because we did not recognize that the reaction with uncomplexed FFA was dependent on vesicle concentration.

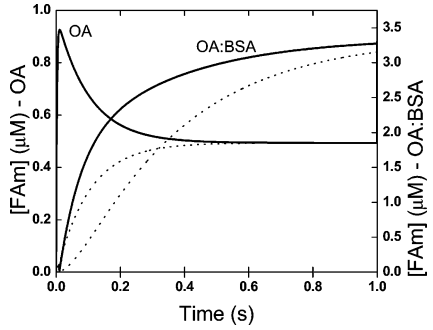

FIGURE 9: Simulations of influx with uncomplexed and complexed oleate. Simulations using eqs 1−5 in Appendix A were solved by Runge−Kutte methods. The following (SUV) parameters were used: $k_{ff} = 5\ s^{-1}$, $k_{off} = 10\ s^{-1}$, $k_{on} = 4 \times 10^6\ M^{-1}\ s^{-1}$, 100 μM SUV, 200 μM BSA, k_{on}(BSA) $= 3 \times 10^7\ M^{-1}\ s^{-1}$, and k_{off}(BSA) $= 1\ s^{-1}$. The initial OA_u concentration for OA complexed with BSA was 60 nM and for uncomplexed OA was 1 μM. The thicker lines are results for uncomplexed OA; the solid lines are the time courses for filling the outer hemileaflet and the dotted lines the inner hemileaflet.

transfer. Intervesicle transfer rate constants measured by Zhang *et al.* (*21*) are virtually identical to the values for flip-flop from the study presented here, consistent with flip-flop as the rate-limiting step for transport. Third, we showed that pH-jump measurements cannot represent rapid flip-flop because they are independent of FFA; they yield the same result with or without FFA (Figure 7). We conclude that the three types of experiments used previously to infer fast transport of FFA across lipid vesicles do not provide information about FFA flip-flop.

Oleate-Mediated Perturbation of Vesicle Bilayers. Results of this study suggest that measurements with uncomplexed OA are affected by a perturbation of the bilayer that effectively allows the fatty acid to bypass the flip-flop step. Our results suggest that perturbation of the influx mechanism results from a combination of stopped-flow mixing and elevated levels of OA_u. Influx measured by stopped-flow mixing with uncomplexed OA reflects binding rather than flip-flop (Figure 6), while slow mixing yields influx rates approaching those obtained with OA−BSA complexes. Moreover, even with BSA present, influx rate constants increase with an increase in OA_u concentration for sufficiently high OA_u concentrations (Figure 2). A possible explanation for the perturbation is provided by simulations of influx that reveal much faster loading of the outer hemileaflet with uncomplexed OA than with the OA−BSA complex (Figure 9). Although the OA−BSA complexes also reveal outer and/or inner asymmetry, this develops more slowly than for uncomplexed OA, suggesting that a rapid and transient OA asymmetry across the bilayer may contribute to vesicle perturbation. The perturbation may be augmented by the hydrodynamic forces generated during rapid stopped-flow mixing and/or rapid loading of the vesicles, as suggested by the lack of fast influx observed in slow mixing with uncomplexed OA.

Flip-Flop Is the Rate-Limiting Step for the Transport of Oleate across Lipid Vesicles. The observed rate constants (k_{in}, k_{out}, and k_{trns}) in this study demonstrate that flip-flop rather than dissociation is the rate-limiting step for the transport of oleate through SUV as well as GUV and that both flip-flop and dissociation rate constants are significantly faster in SUV than in GUV (Table 1). As discussed in the Appendix and previously (*12*), dissociation of OA from OA−BSA complexes is not rate limiting under the conditions described in this study. However, the buffering of OA_u concentration by the OA−BSA complexes leads to a somewhat surprising result; under conditions in which the OA_u concentration is well-buffered, the rate constants for binding and influx are predicted to be less than k_{off} for slow k_{ff} and approach $k_{off}/2$ at infinite k_{ff} (Appendix). We also determined that the intrinsic rate constants, those corresponding to the model discussed in the Appendix, are consistent with slow flip-flop. This was done by fitting simultaneously the time courses for influx, efflux, and transfer using MLAB. The results are consistent with the pattern of the observed rate constants ($k_{in} \approx k_{out} < k_{trns}$) but indicate that the difference between k_{ff} and k_{off} is even greater than that between the corresponding observed rates.

We conclude that flip-flop is the rate-limiting step for the transport of oleic acid and probably other long chain FFA across lipid bilayers. These results strongly suggest that the lipid phase should also present a significant barrier to FFA transport across biological membranes. Whether protein transporters are needed to overcome this barrier would depend on the nature of the barrier and the metabolic requirements of the specific cell. Rate constants for flip-flop across erythrocyte ghost membranes (*12*), measured using FFA−BSA complexes, are quite similar to the values obtained in this study for GUV. On the other hand, evidence from measurements of transport across adipocytes, using FFA−BSA complexes, indicates that FFA transport rates are at least 1 order of magnitude lower than those observed for erythrocyte ghosts or lipid vesicles (*22*). This suggests that the barrier for FFA transport may be a sensitive function of the composition of the lipid phase of biological membranes.

ACKNOWLEDGMENT

We thank Dr. Wylie Nichols for important comments that have helped to clarify the manuscript.

APPENDIX

Vesicle Transport Model. Herein we describe the kinetic models corresponding to the kinetic pathways for the transport of OA using OA−BSA complexes (**I**) and for uncomplexed OA (**II**). Not shown are the hydrogen binding and dissociation steps, which are likely rapid compared to the other kinetic steps.

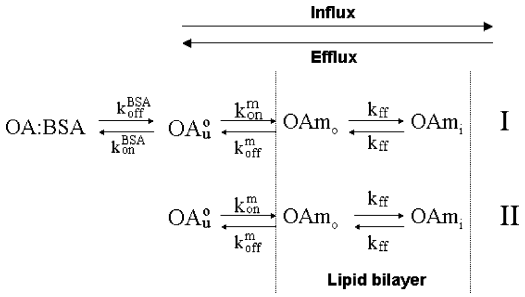

The quantities OA_u^o, OAm_o, and OAm_i are concentrations of the extravesicular unbound OA and OA bound in the outer and inner hemileaflets of the vesicle, respectively.

The time courses for movement of FFA into and out of vesicles were simulated with kinetic models similar to those used previously (*11*, *12*). The models were used to investigate the effect of the method of FFA addition, either complexed with BSA (**I**) or uncomplexed (**II**), and to obtain the model rate constants by fitting to the measured time courses. Equations 1−5 represent the model for the BSA complex with a general FFA and were solved using Macsyma version 2.4 or MLAB.

$$\frac{d[BSA_b]}{dt} = k_{on}^{BSA}([BSA_T] - [BSA_b])[FFA_o] - k_{off}^{BSA}[BSA_b] \quad (1)$$

$$\frac{d[FFA_o]}{dt} = k_{off}^{M}[FAm_o] + k_{off}^{BSA}[BSA_b] - k_{on}^{M}L[FFA_o] - k_{on}^{BSA}([BSA_T] - [BSA_b])[FFA_o] \quad (2)$$

$$\frac{d[FAm_o]}{dt} = k_{on}^{M}L[FFA_o] - k_{off}^{M}[FAm_o] + k_{ff}([FAm_i] - [FAm_o]) \quad (3)$$

$$\frac{d[FAm_i]}{dt} = k_{ff}([FAm_o] - [FAm_i]) \quad (4)$$

In these equations, $[BSA_T]$, $[BSA_b]$, $[FFA_o]$, $[FFA_i]$, $[FAm_o]$, $[FAm_i]$, and L are the concentrations of total and bound BSA, outside and inside FFA, and bound fatty acid (FA) in the outer and inner hemileaflets of the vesicle and the vesicle (phospholipid) concentration, respectively. The rate constants denoted with M and BSA are those for the membrane vesicles and BSA, respectively, and k_{ff} is the flip-flop rate constant. BSA's six binding sites for FFA are assumed to be independent and have equal affinities (15 nM), consistent with measurements that reveal no dependence of dissociation rate constants on the ratio of FFA to BSA (*23*). Therefore, for these simulations (eqs 1 and 2), $[BSA_T]$ and $[BSA_b]$ represent the concentrations of FFA binding sites.

For mixing uncomplexed FFA, the model consists of eqs 3 and 4 with eqs 1 and 2 replaced by eq 5

$$\frac{d[FFA_o]}{dt} = k_{off}^{M}[FAm_o] - k_{on}^{M}L[FFA_o] \quad (5)$$

Simulations of Influx with the OA−BSA Complex. Simulations of influx using OA−BSA complexes were done using eqs 1−4 for a range of BSA dissociation rate constants (k_{off}^{BSA}), vesicle concentrations of 10 and 100 μM, a BSA_T concentration of 50 μM, a k_{ff} of 5 s^{-1}, and a k_{off}^{M} of 15 s^{-1}. Rate constants for OA binding and transport were estimated from the FAm_o and FAm_i concentration time courses, respectively. The results indicate that for well-buffered conditions the rate of binding is virtually independent of k_{off}^{BSA} and is significantly faster than the rate of influx (Table 2). This lack of dependence on k_{off}^{BSA} simply reflects the fact that for well-buffered OA_u the fraction of OA that dissociates from BSA is negligible (*12*).

In addition, results of simulations reveal important features of binding and influx for the BSA-buffered system (constant FFA_o concentration). In the limit that k_{ff} approaches zero, the rate constant for binding approaches k_{off}^{M}. This can be seen by solving eq 3 with a k_{ff} of 0, which, for a constant FFA_o concentration, yields

$$[FAm_o](t) = \frac{k_{on}^{M}L[FFA_o]}{k_{off}^{M}}(1 - e^{-k_{off}^{M}t}) \quad (6)$$

For infinite k_{ff}, an analytical solution to eqs 3 and 4 reveals a rate constant for binding and influx of $k_{off}^{M}/2$, and simulation of eqs 1−4 reveals an approximately 15% smaller limit.

Simulations of influx time courses with uncomplexed oleate for a range of vesicle concentrations and fixed rate constants reveal that binding rate constants range from ∼5 to 700 s^{-1} for vesicle concentrations from 5 to 100 μM (Figure 9). These values are more than 20-fold faster (for 100 μM) than for OA−BSA complexes and, in contrast to the lack of vesicle concentration dependence for OA−BSA complexes, reveal a linear increase in binding rate constants with vesicle concentration. This linear dependence on vesicle concentration can be derived by approximating eq 3 at early times and reveals a solution with a rate constant equal to $k_{off} + k_{on}$[vesicle]. The time course for the FAmo concentration (Figure 9) is a reflection of the rapid loading of the vesicles followed by slow depletion by flip-flop and off rate. Shortly after being mixed with uncomplexed OA, the bilayer reveals significant outer vs inner hemileaflet asymmetry, which contrasts with the slowly developed asymmetry for OA−BSA complexes.

Table 2: Effect of BSA Rate Constants on Rate Constants for Binding to Vesicles[a]

k_{off}^{BSA} (s^{-1})	$k_{binding}$ (s^{-1})	
	$L = 10\ \mu M$	$L = 100\ \mu M$
0.5	11.7	9.1
1.0	11.7	10.5
2.0	11.7	11.3
4.0	12.08	11.7

[a] Simulations were done using eqs 1−4 of the Appendix with the following parameters: $k_{off}^{M} = 15\ s^{-1}$, $k_{ff} = 5\ s^{-1}$, $k_{off}^{BSA}/k_{on}^{BSA}$ fixed at 32 nM, 50 μM BSA, 150 μM OA_T (3:1), and lipid (L) concentrations of 10 or 100 μM.

REFERENCES

1. Hamilton, J. A., and Kamp, F. (1999) How are free fatty acids transported in membranes, *Diabetes 48*, 2255−2269.
2. Zakim, D. (2000) Thermodynamics of fatty acid transfer, *J. Membr. Biol. 176*, 101−109.
3. Kleinfeld, A. M. (2000) Lipid phase fatty acid flip flop, is it fast enough for cellular transport? *J. Membr. Biol. 175*, 79−86.
4. Watkins, P. A., Hamilton, J. A., Leaf, A., Spector, A. A., Moore, S. A., Anderson, R. E., Moser, H. W., Noetzel, M. J., and Katz, R. (2001) Brain uptake and utilization of fatty acids: applications to peroxisomal biogenesis diseases, *J. Mol. Neurosci. 16*, 87−92.
5. Daniels, C., Noy, N., and Zakim, D. (1985) Rates of Hydration of Fatty Acids Bound to Unilamellar Vesicles of Phosphatidylcholine or to Albumin, *Biochemistry 24*, 3286−3292.
6. Kamp, F., and Hamilton, J. A. (1992) pH gradients across phsopholipid membranes caused by fast flip-flop of un-ionized fatty acids, *Proc. Natl. Acad. Sci. U.S.A. 89*, 11367−11370.
7. Kamp, F., Zakim, D., Zhang, F., Noy, N., and Hamilton, J. A. (1995) Fatty acid flip-flop in phospholipid bilayers is extremely fast, *Biochemistry 34*, 11928−11937.

8. Srivastava, A., Singh, S., and Krishnamoorthy, G. (1995) Rapid transport of protons across membranes by aliphatic amines and acids, *J. Phys. Chem. 99*, 11302−11305.
9. Thomas, R. M., Baici, A., Werder, M., Schulthess, G., and Hauser, H. (2002) Kinetics and mechanism of long-chain fatty acid transport into phosphatidylcholine vesicles from various donor systems, *Biochemistry 41*, 1591−1601.
10. Pohl, E. E., Peterson, U., Sun, J., and Pohl, P. (2000) Changes of Intrinsic Membrane Potentials Induced by Flip-Flop of Long-Chain Fatty Acids, *Biochemistry 39*, 1834−1839.
11. Kleinfeld, A. M., Chu, P., and Romero, C. (1997) Transport of long chain native fatty acids across lipid bilayer membranes indicates that transbilayer flip-flop is rate limiting, *Biochemistry 36*, 14146−14158.
12. Kleinfeld, A. M., Storms, S., and Watts, M. (1998) Transport of long chain fatty acids across human erthrocyte ghost membranes, *Biochemistry 37*, 8011−8019.
13. Richieri, G. V., Ogata, R. T., and Kleinfeld, A. M. (1992) A fluorescently labeled intestinal fatty acid binding protein; Interactions with fatty acids and its use in monitoring free fatty acids, *J. Biol. Chem. 267*, 23495−23501.
14. Kleinfeld, A. M., Chu, P., and Storch, J. (1997) Flip-flop is slow and rate limiting for the movement of long chain anthroyloxy fatty acids across lipid vesicles, *Biochemistry 36*, 5702−5711.
15. Gomori, G. (1942) A modification of the colorimetric phosphorus determination for use with the photoelectric colorimeter, *J. Lab. Clin. Med. 27*, 955−960.
16. Richieri, G. V., Ogata, R. T., and Kleinfeld, A. M. (1999) The measurement of free fatty acid concentration with the fluorescent probe ADIFAB: A practical guide for the use of the ADIFAB probe, *Mol. Cell. Biochem. 192*, 87−94.
17. Massey, J. B., Bick, D. H., and Pownall, H. J. (1997) Spontaneous transfer of manoacyl amphiphiles between lipid and protein surfaces, *Biophys. J. 72*, 1732−1743.
18. Anel, A., Richieri, G. V., and Kleinfeld, A. M. (1993) Membrane partition of fatty acids and inhibition of T cell function, *Biochemistry 32*, 530−536.
19. Barreto, J., and Lichtenberger, L. M. (1992) Vesicle acidification driven by a millionfold proton gradient: a model for acid influx through gastric cell membranes, *Am. J. Physiol. 262*, G30−G34.
20. Peitzsch, R. M., and McLaughlin, S. (1993) Binding of acylated peptides and fatty acids to phospholipid vesicles: pertinence to myristoylated proteins, *Biochemistry 32*, 10436−10443.
21. Zhang, F., Kamp, F., and Hamilton, J. A. (1996) Dissociation of long and very long chain fatty acids from phospholipid bilayers, *Biochemistry 35*, 16055−16060.
22. Kampf, J. P., and Kleinfeld, A. M. (2002) Fatty acid influx and efflux in adipocytes monitored by imaging intracellular FFA, *Biophys. J.*, 562a.
23. Demant, E. J. F., Richieri, G. V., and Kleinfeld, A. M. (2002) Stopped-flow kinetic analysis of long-chain fatty acid dissociation from bovine serum albumin, *Biochem. J. 363*, 809−815.

BI036335L